Available online at www.sciencedirect.com
SCIENCE DIRECT®
Food Chemistry 94 (2006) 179–192
Food Chemistry
www.elsevier.com/locate/foodchem

Microstructure changes of sodium carbonate-soluble pectin of peach by AFM during controlled atmosphere storage

Hong-Shun Yang [a,b], Guo-Ping Feng [b], Hong-Jie An [c], Yun-Fei Li [b,*]

[a] Institute of Refrigeration and Cryogenics Engineering, Shanghai Jiao Tong University, Shanghai 200030, PR China
[b] Department of Food Science and Technology, Shanghai Jiao Tong University, 2678 Qixin Road, Shanghai 201101, PR China
[c] Nanobiology Laboratory, Shanghai Jiao Tong University, Shanghai 200030, PR China

Received 17 May 2004; received in revised form 8 November 2004; accepted 8 November 2004

Abstract

Yellow peaches (*Prunus persicu* L. Batsch.) were stored under controlled atmospheres (CA) of 2%O_2 + 5%CO_2, 5%O_2 + 10%CO_2, 2%O_2 + 10%CO_2, 5%O_2 + 5%CO_2, and normal atmosphere at 2 °C, to investigate the effects of different concentrations of O_2 and CO_2 on the structure of a single sodium carbonate-soluble pectin (SSP) molecule. The microstructure changes, including aggregates and branches, were studied by atomic force microscopy (AFM) at initially, on the 15th and 45th day. The microstructure of SSP molecules and polymers showed that aggregates separated gradually with the storage time. The degradation took place in the linear backbone as well as in side chains. The degradation of SSP molecules was inhibited by lower O_2 and higher CO_2 concentrations. Almost all of the chains were composed of four basic units with widths of 11.719, 15.625, 19.531 and 17.578 nm, which can be visualized and calculated exactly by AFM. This indicated that parallel linkage or intertwist between the basic units was a fundamental characteristic of SSP molecules.

Keywords: Peach; Atomic force microscopy; Controlled atmosphere storage; Pectin; Structure

1. Introduction

Plant pectin is a very important foodstuff and also an additive for food products. It is a family of complex galacturonic acid-rich polysaccharides present in the primary cell wall and intercellular spaces of higher plants (Limberg et al., 2000a). Its common components are homogalacturonan (HG), rhamnogalacturonanI (RGI), rhamnogalacturonan II (RG II) and xylogalacturonan. The functional properties of pectin, at both harvest and postharvest times, are closely related to its chemical and physical structures. Classical methods, such as NMR (Golovchenko, Ovodova, Shashkov, & Ovodov, 2002), enzyme analysis (Limberg et al., 2000a, 2000b) and biochemical analyses (Willats et al., 2000) were used to investigate the structures.

The degradation of pectin is important for commercial applications (Ridley, O' Neill, & Mohnen, 2001). However, since pectin is a heterogeneous structure, it is hard to study. Varied structures or complex repeat units are difficult to determine due to the irregular sequences and have to be averaged across the whole sample.

Atomic force microscopy (AFM) affords an opportunity to directly image individual pectin molecules and polymers. Sodium carbonate-soluble pectin (SSP) from unripe tomato (Round, MacDougall, Ring, & Morris, 1997; Round, Rigby, MacDougall, Ring, & Morris, 2001), from alginate and gel (Decho, 1999); from biopolymers (Morris et al., 2001); from *iota*-carrageenan (Gunning et al., 1998) and from cell wall (Fahlén & Salmén, 2003; Kunzek, Kabbert, & Gloyna, 1999) has

* Corresponding author. Tel./fax: +86 21 6478 3085.
E-mail addresses: hsyang@sjtu.edu.cn (H.-S. Yang), yfli@sjtu.edu.cn (Y.-F. Li).

0308-8146/$ - see front matter © 2005 Published by Elsevier Ltd.
doi:10.1016/j.foodchem.2004.11.003

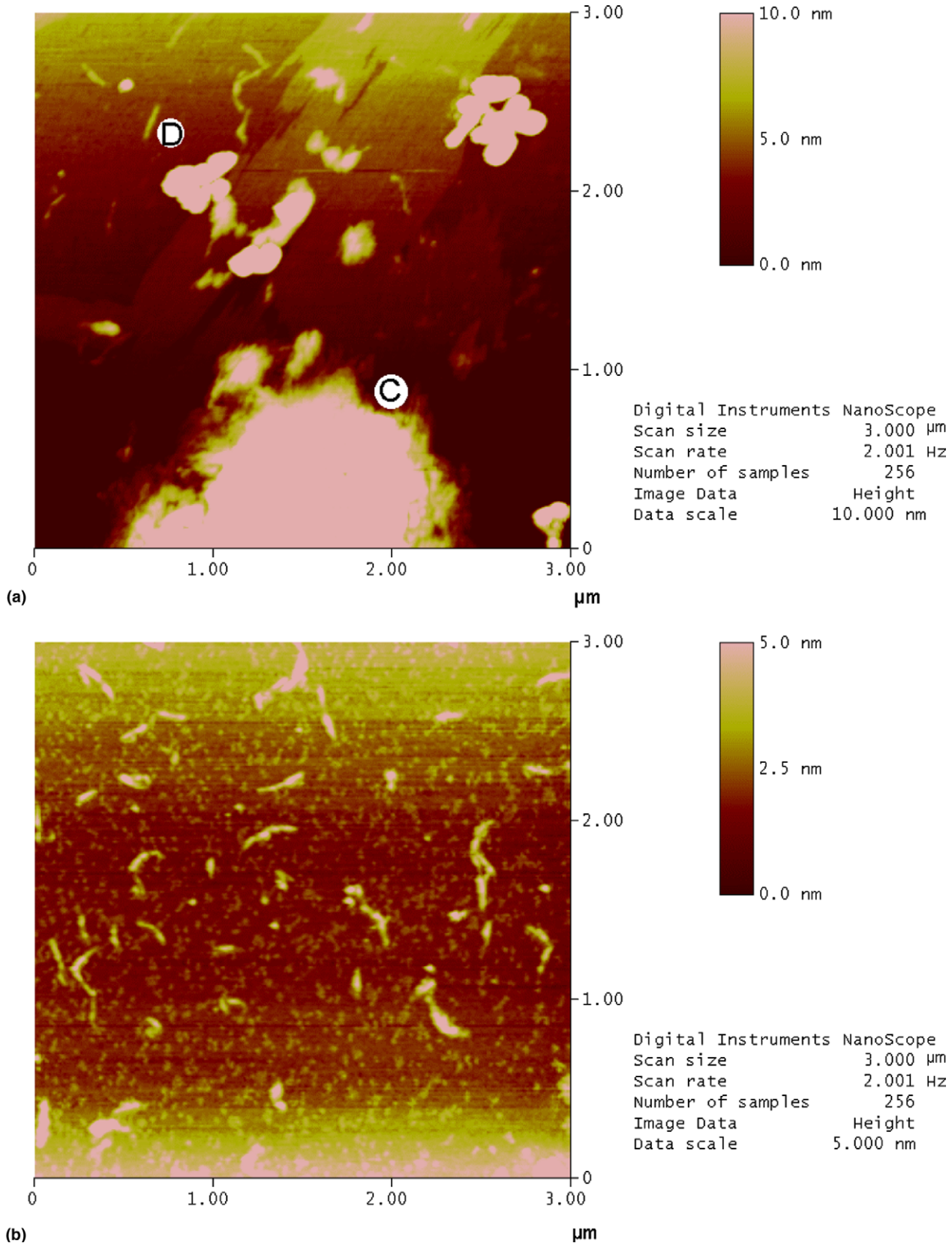

Fig. 1. AFM images of sodium carbonate-sodium pectin of fresh peach: (a) typical image; (b) atypical image. Note: C, linear single fraction; D, polymer.

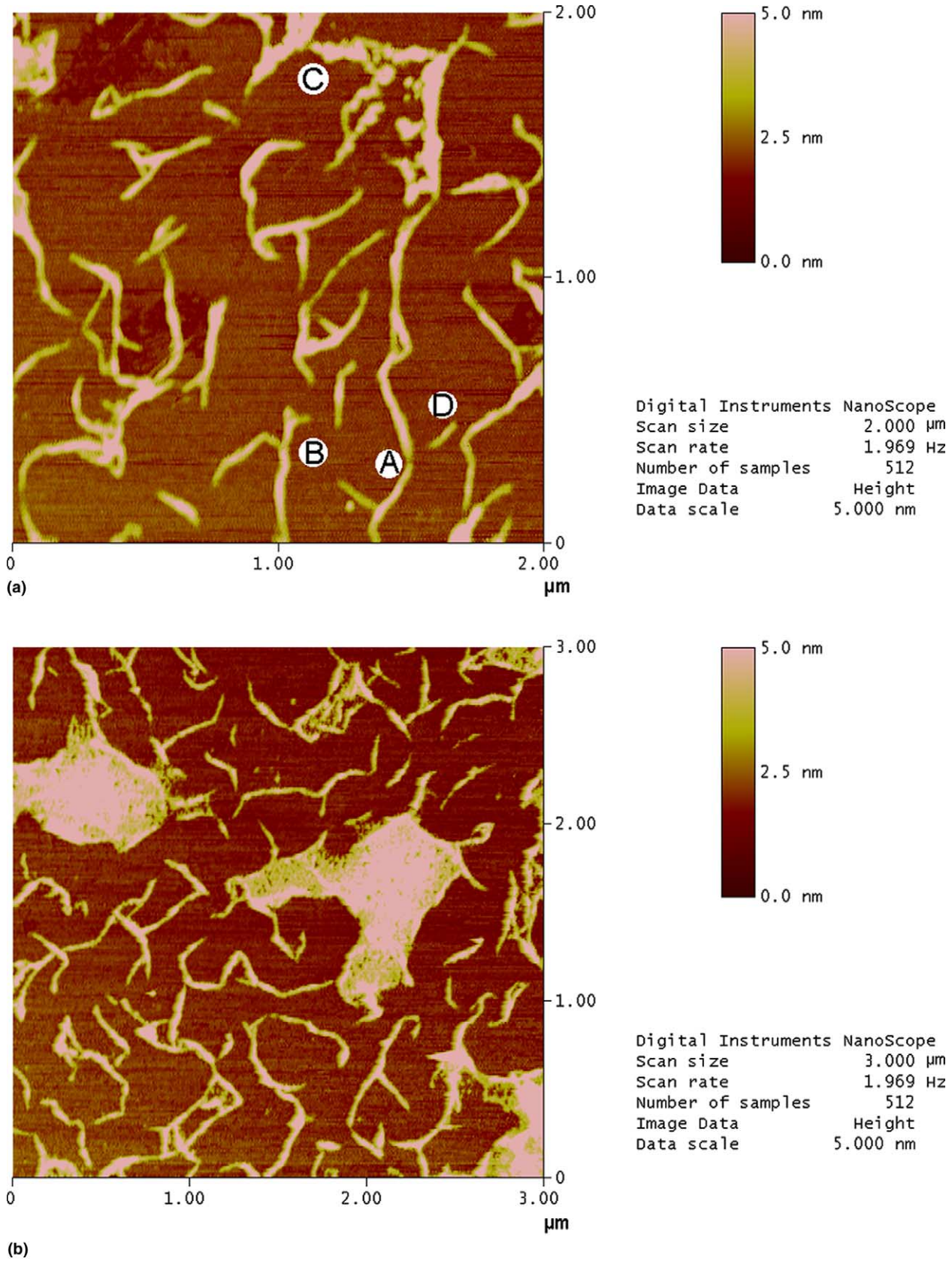

Fig. 2. AFM images of SSP of peach on the 15th day under CA1 to CA4 storage: (a) CA1; (b) CA2; (c) CA3; (d) CA4. Note: A, cleavage point; B, branch; C, linear single fraction; D, polymer.

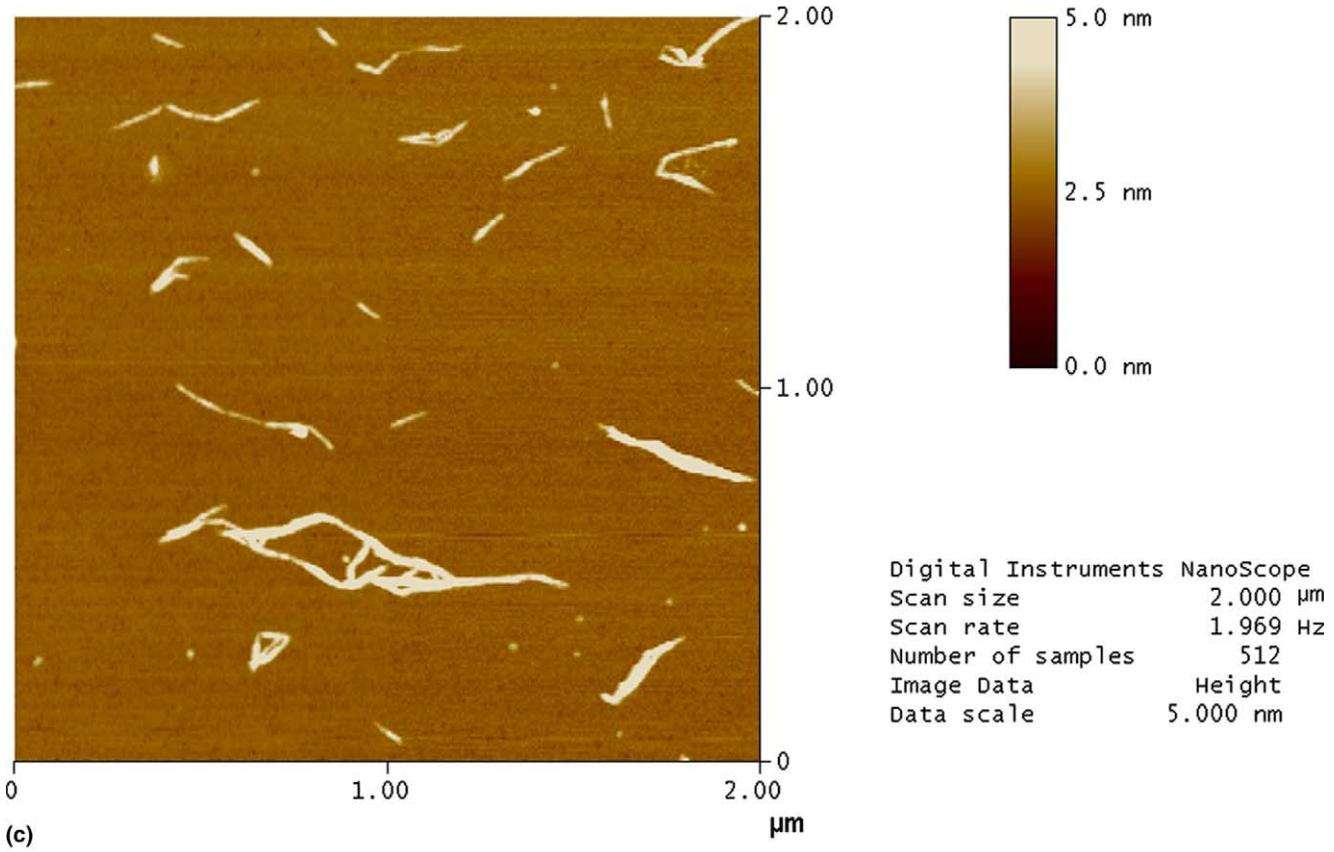

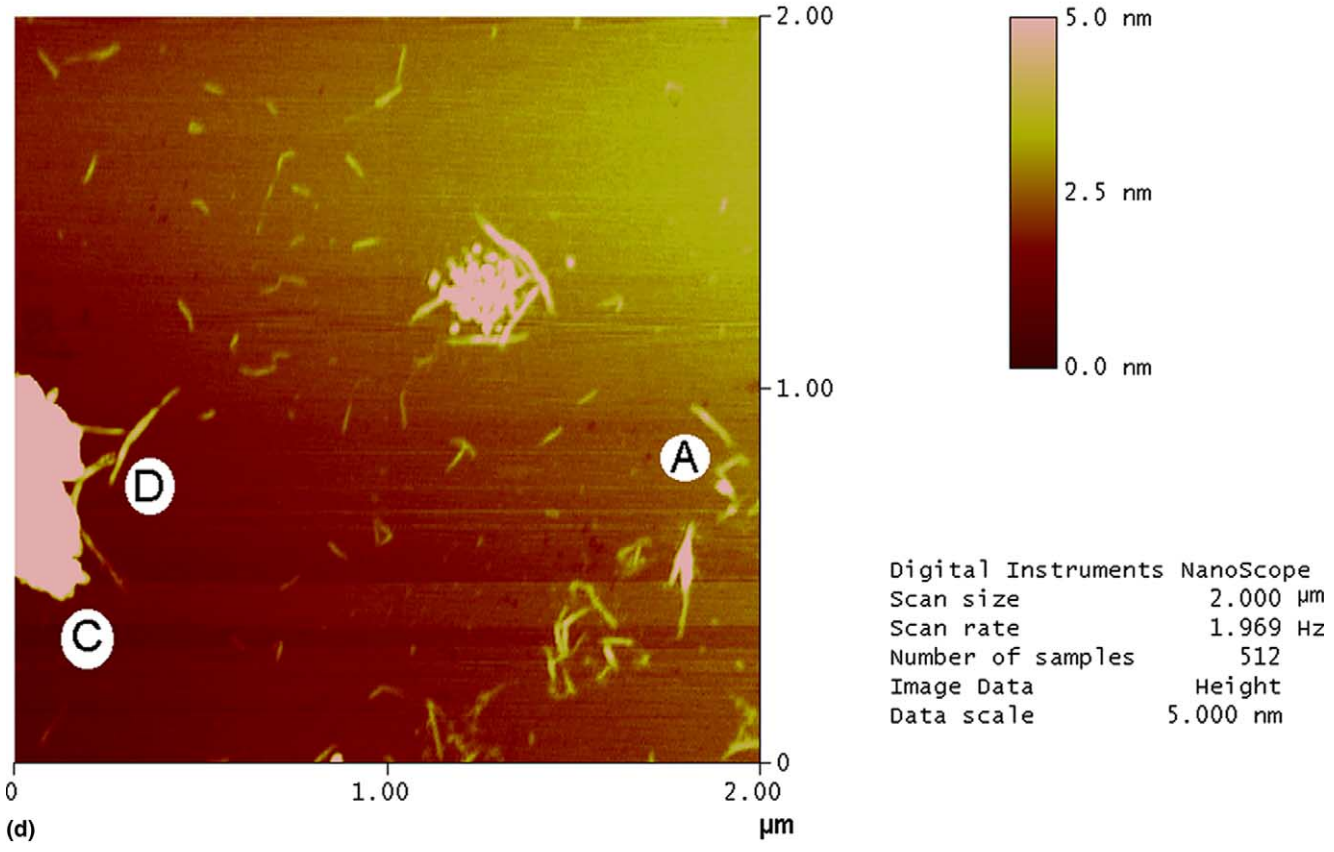

Fig. 2 (*continued*)

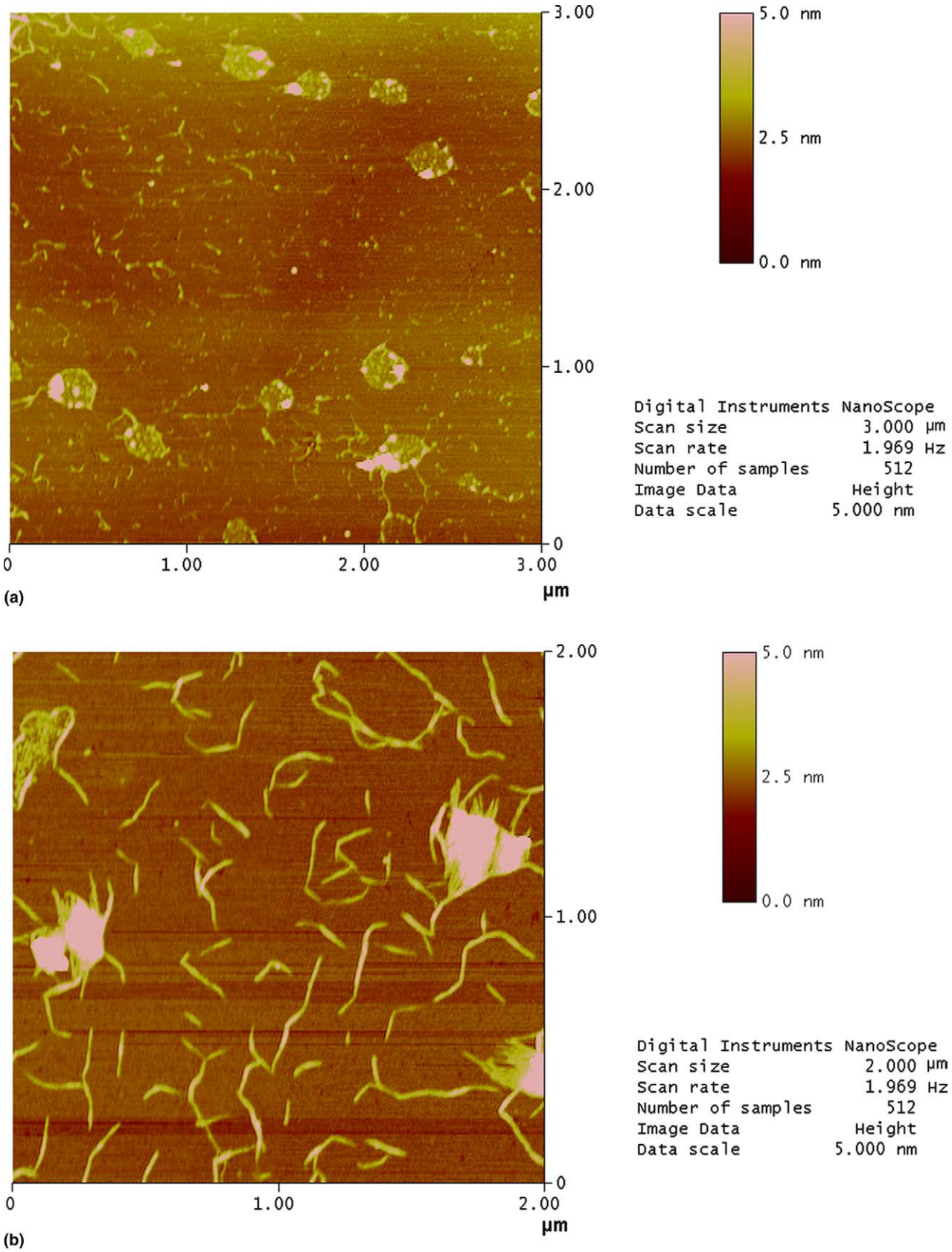

Fig. 3. AFM images of SSP of peach on the 15th day under normal atmosphere storage: (a) typical image; (b) localized image; (c) enlargement image of SSP. Note: A, cleavage point; B, branch; C, linear single fraction; D, polymer.

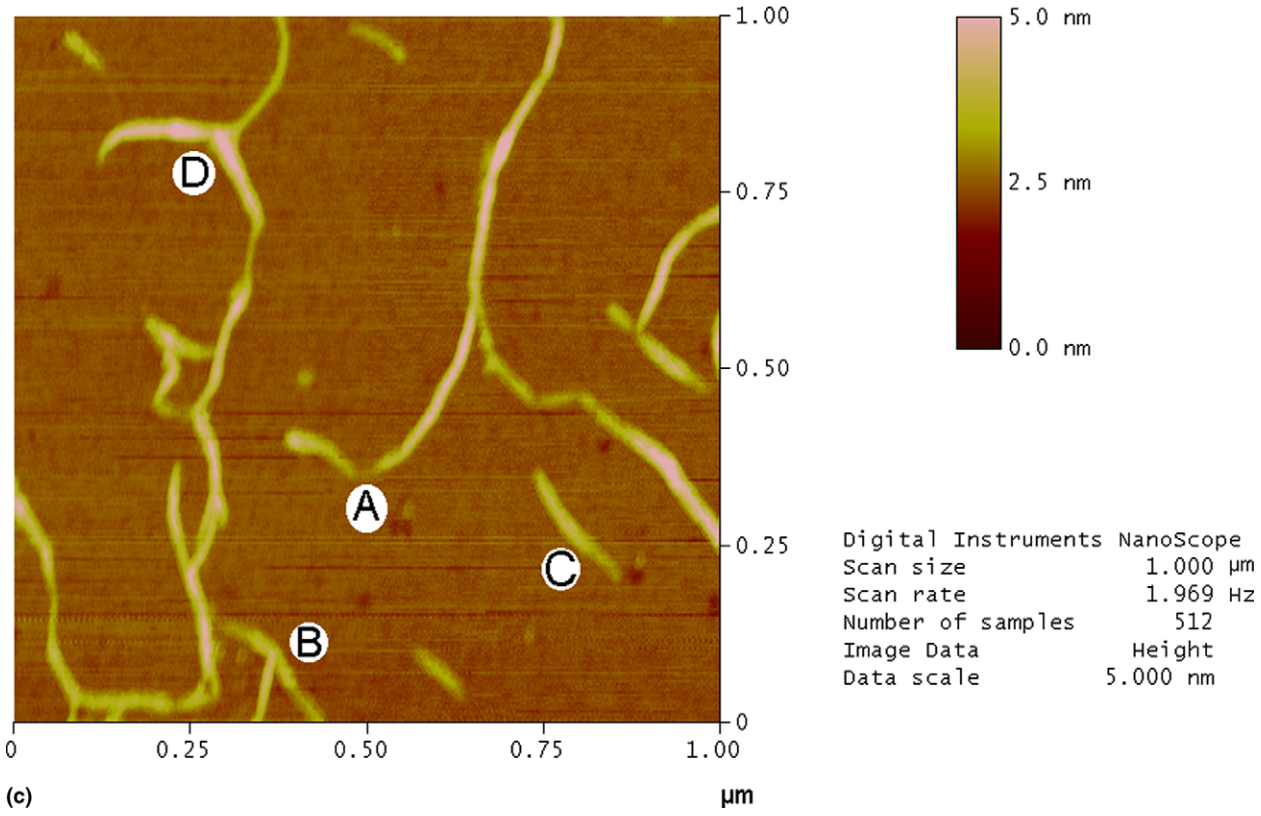

Fig. 3 (*continued*)

been studied by AFM. The molecular branching, molecular mass distributions, interactions involved in supra-molecular assembly and cell wall structure and polysaccharide gelatin have been illustrated.

Controlled atmosphere (CA) storage can help in maintaining high quality of produce, including firmness (Fernández-Trujillo, Cano, & Artés, 2000). Texture is considered to be related to pectin (Chang, Lai, & Chang, 1995; Tijskens, Rodis, Herbog, Kalantzi, & Dijk, 1998). However, there is no report about the degradation of pectin under CA storage by AFM. To investigate and further illustrate the effect of enzymes on pectin, and to compare with enzymatic research (Limberg et al., 2000a, 2000b; Willats et al., 2000), we chose SSP as an analysis object as it may relate to complex reactions and is not uneasily studied by chemical methods.

The overall goal of this study was to examine the morphological arrangement of peach SSP, and its changes during CA storages. The degradation mechanism of the peach pectin was also studied by AFM images.

2. Materials and methods

2.1. Fruits

Yellow peaches (*Prunus persicu* L. Batsch.), at commercial maturity according to acceptable colour standards but at a pre-climacteric stage, were harvested from an orchard in Fengxian, Shanghai city, China. The fruits were transported to a laboratory within 2 h and immediately pre-cooled (4 °C, 12 h). After that they were stored at 2 ± 1 °C and ready for tests.

2.2. Storage conditions

Storage conditions were as follows:

CA1, 2% O_2 + 5% CO_2; CA2, 5% O_2 + 10% CO_2; CA3, 2% O_2 + 10% CO_2; CA4, 5% O_2 + 5% CO_2 and CA5, normal atmosphere. Five controlled atmosphere cabinets (105 cm × 55 cm × 100 cm), with 5 CO_2 absorbers (Soda lime containing ethyl violet as indicator) and 5 ethylene absorbers were connected to an atmosphere analyzer (GAC 1100, Italy). The initial concentrations of O_2 and CO_2 in the CA1 to CA4 cabinets were established by control of flow rate of N_2 generated by cellulose membrane and CO_2 via pressure regulators. There were 120 ± 10 kg of peaches in each CA cabinet and all treatments were at 2 ± 1 °C with approximately 95% RH.

2.3. Sodium carbonate-soluble pectin extraction

The SSP was extracted according to the method of Zhou et al. (2000) with slight modification. Peaches, taken from CA1 to CA5, were peeled and about 5.5 g flesh from each condition were used for extraction

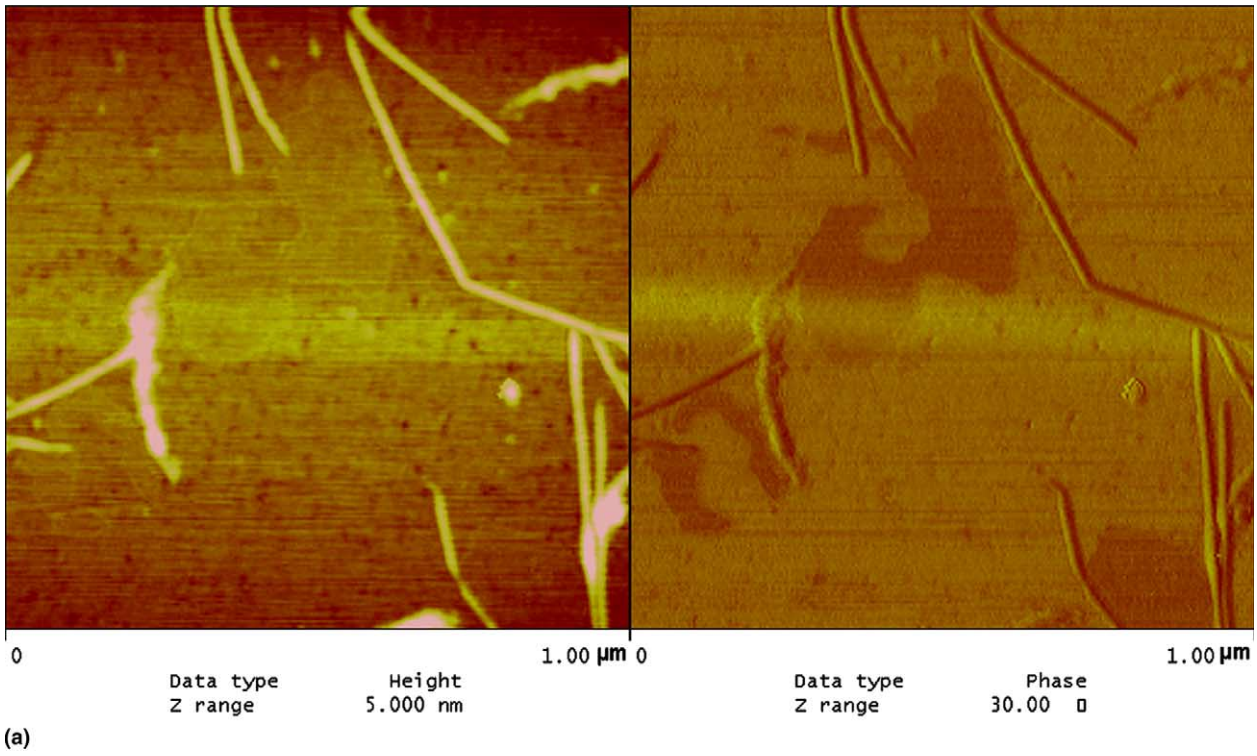

Fig. 4. AFM images of SSP of peach on the 45th day under CA1 and CA2 storage: (a) CA1, phase mode; (b) CA2, phase mode; (c) CA2, general image; (d) CA2, unexpected image. Note: T: triangular branched structure.

of cell wall material. The fleshes were boiled in ethanol for 20 min, then the ethanol was decanted by filtration, and the solid residue was transferred to 20 ml ultra-purified water (Milli-Q Biocel Pure Water Equipment, Millipore Co. Ltd., France). After 2 h extraction, supernatant was collected and the pellet was

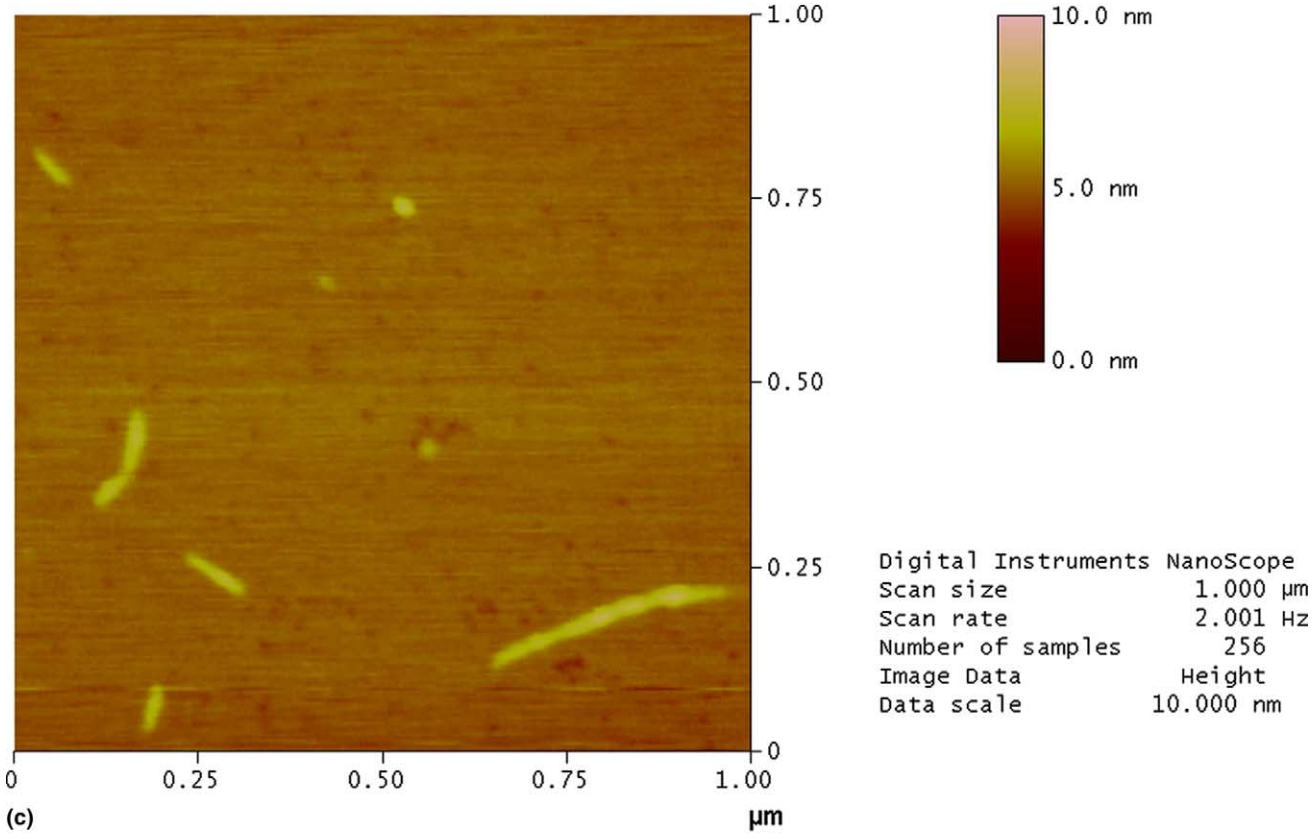

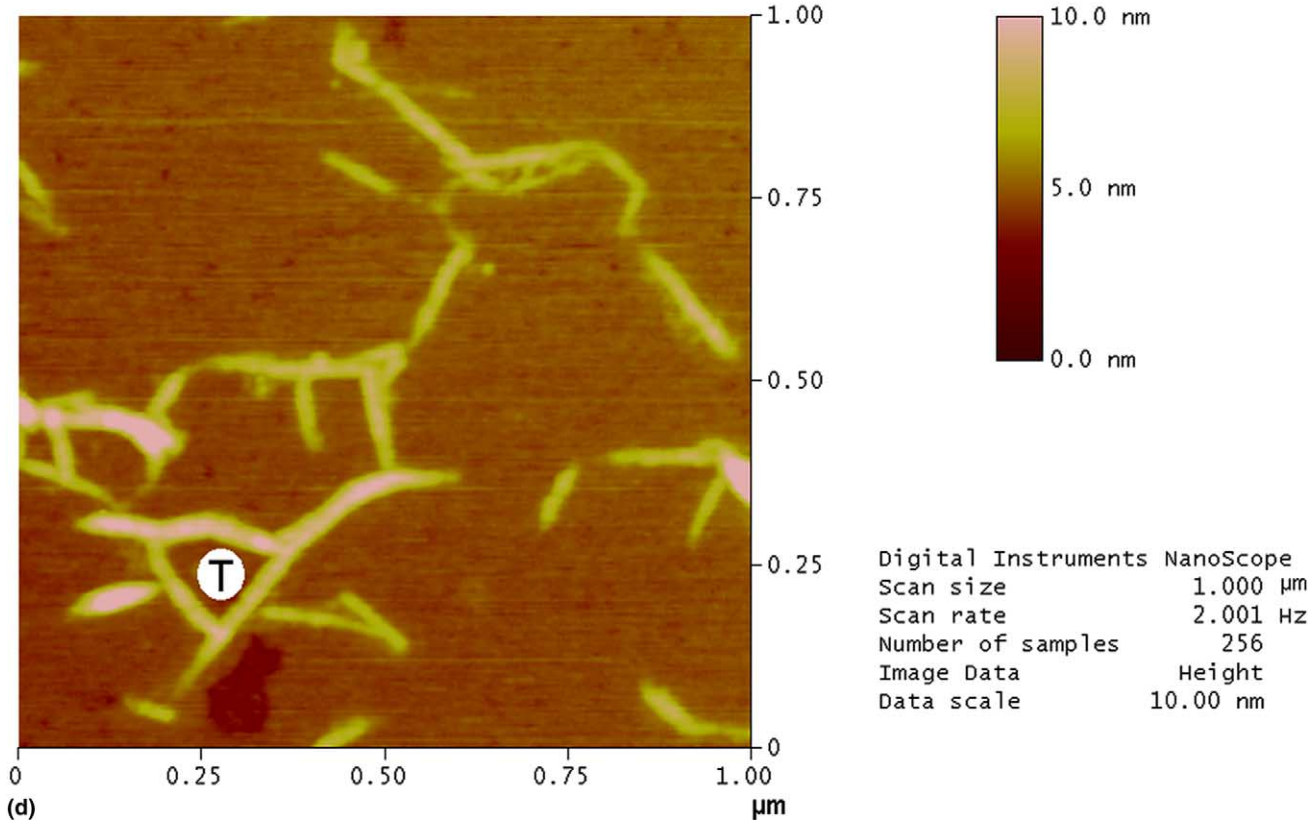

Fig. 4 (*continued*)

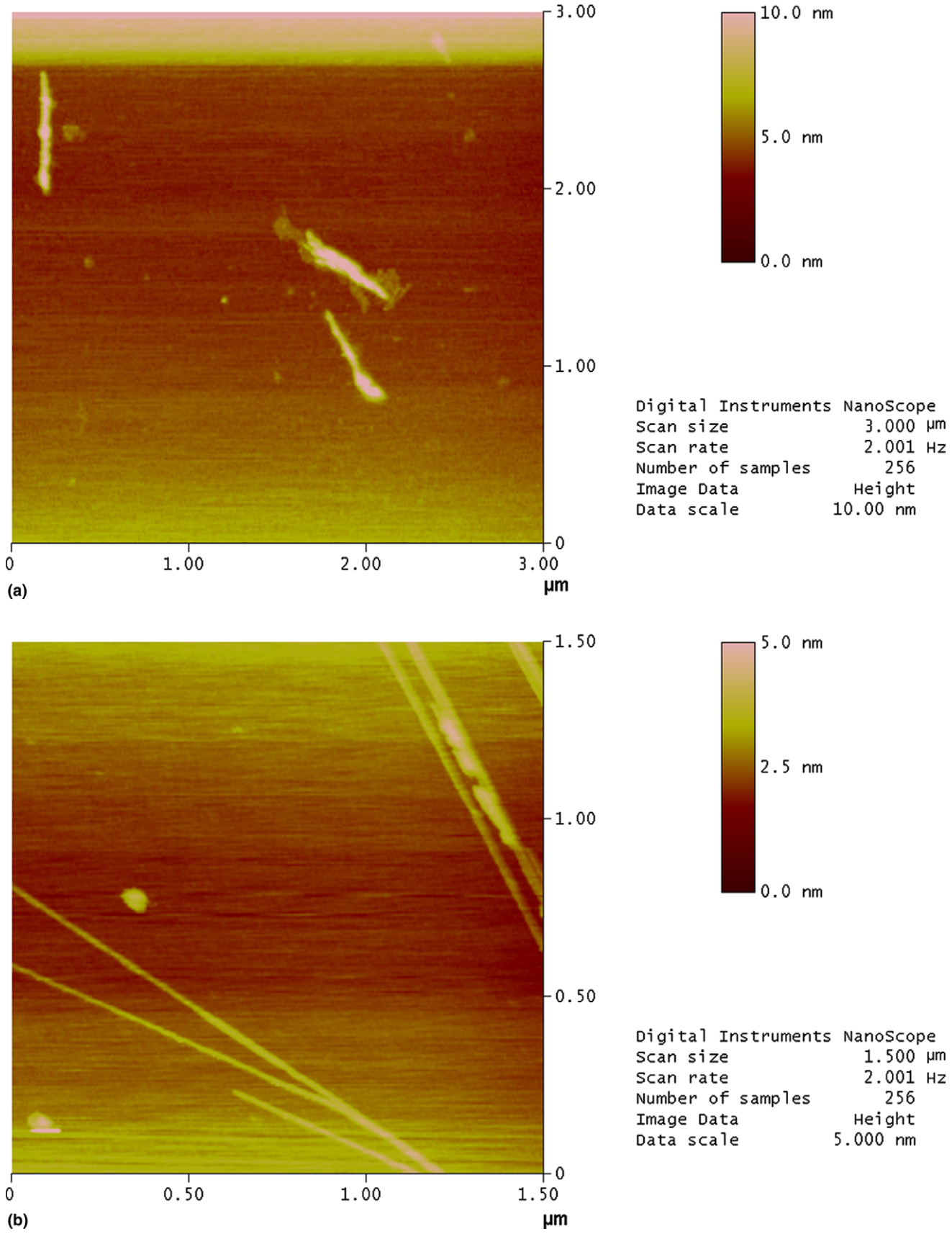

Fig. 5. AFM images of SSP of peach on the 45th day under CA3 to CA5 storage: (a) CA3; (b) CA4; (c) CA5, normal atmosphere.

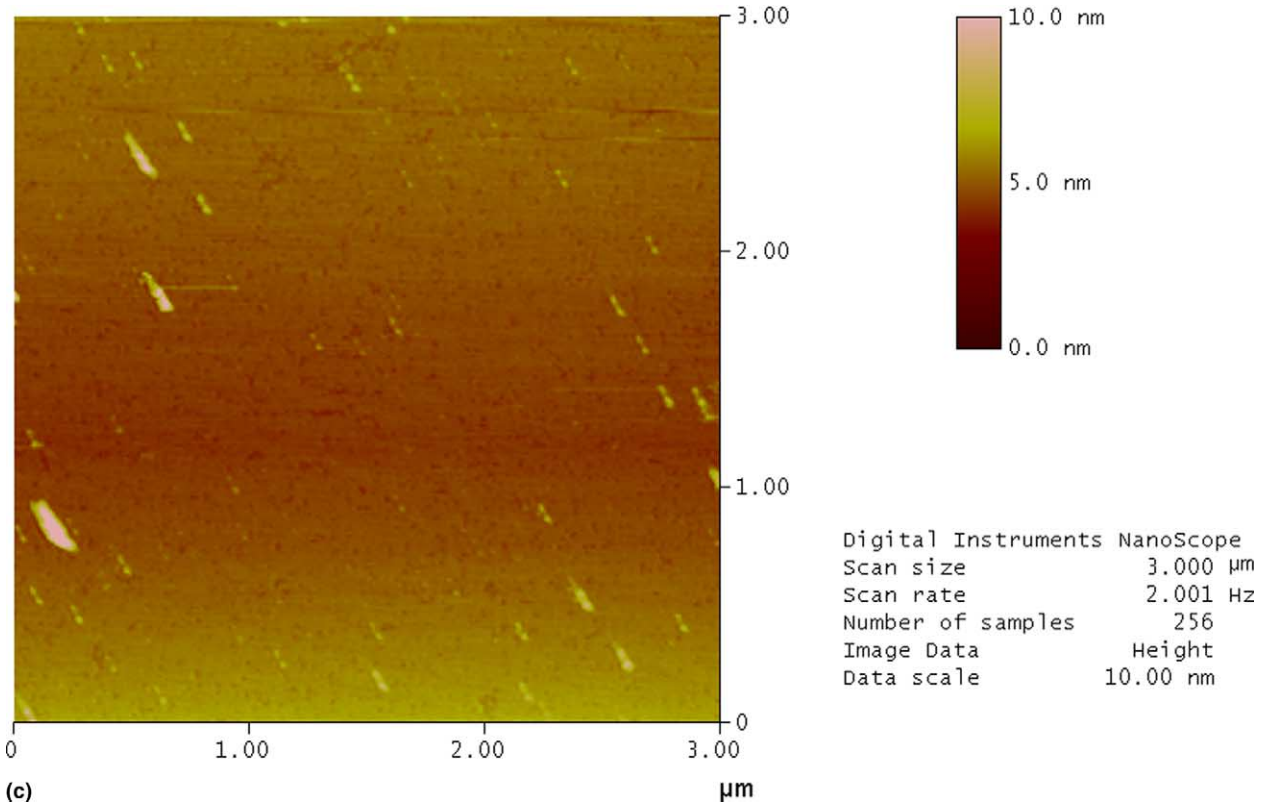

Fig. 5 (*continued*)

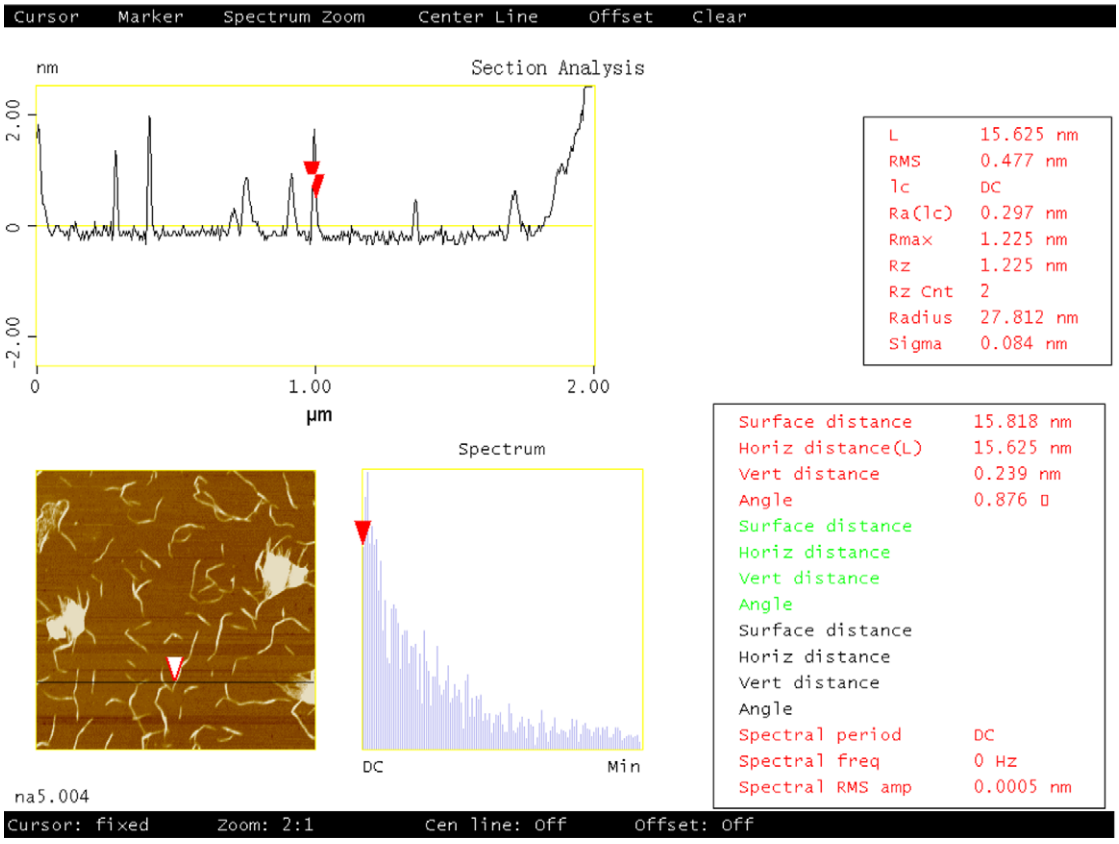

Fig. 6. Cross-section analysis of SSP polymers and single strands on the 15th day under normal atmosphere storage Note: the thickness was determined by height (nm) on the *y*-axis (vertical), Arrows represent markers for width measurements.

washed with acetone, then with chloroform:methanol (1:1 v/v). The pellet was resuspended in 20 ml 50 mM *trans*-1,2-diaminocyclohexane-*N*,*N*,*N*′,*N*′-tetraacetic acid (CDTA), shaken for 3 h and centrifuged (Beijing Medical Equipments Co. Ltd) at 15,000*g* for 10 min, and the supernatant was collected and the pellet was extracted twice more with 10 mM CDTA. The pellet resuspended in 20 ml 50 mM Na_2CO_3 and 20 mM $NaBH_4$ at 4 °C for 18 h, then 2 h at room temperature, was centrifuged at 15,000*g* for 10 min and extracted twice more with 20 ml of Na_2CO_3. Three supernatants were adjusted to pH 7.0 with acetic acid and a fraction was obtained.

2.4. AFM manipulation

The AFM, in a glove box, was manipulated at 30–40% relative humidity (RH) and 23–25 °C. The variation of humidity inside the glove box was controlled by silica gel and the humidity was stabilized for at least 5 h prior to AFM observation (Balnois & Wilkinson, 2002).

Pectin solutions (~1 mg/l) were diluted to 0.5–30 μg/ml in a series of concentrations. To deposit SSP molecules onto newly cleaved sheets of mica, a small volume (20 μl) of solutions was pipetted briefly (~5 s) onto the mica surface, and then quickly removed by pipette. The mica surface was air dried (1 h) in a dust-free enclosure before using the AFM image with Tapping mode at the scan speed of 2 Hz.

Tapping mode was carried out using a multimode NanoScope IIIa AFM (digital instruments Santa Barbara, CA, USA) equipped with a Si_3N_4 cantilevered scanner with a 12×12 μm^2 scan size and a 4 μm vertical range. In the tapping mode AFM, the tip was oscillated with high frequency in the vertical direction and was only intermittently in contact with the sample. It has a high resolution with about 0.1 nm for vertical range and 1–2 nm for lateral (Darrort, Troyon, Ebothé, Bissieux, & Nicollin, 1995).

To make the results comparable, before imaging each sample, the integrity of the AFM tip was verified by imaging a reference standard with a known roughness of 5–7 nm (Reed, Singer, Kresbach, & Schwartz, 1998).

Since AFM images are generally limited to small scanned areas, several images of different zones were examined and offline analyzed with version 5.12 software on each specimen in order to average the results (Darrort et al., 1995). The correction of the images by this software enabled reduction of the noise.

2.5. AFM image analysis

The bright and dark areas in the image corresponded to peaks and troughs in the SSP chains. Different scales were used in the vertical and horizontal scale. Height mode was used for analysis, because phase mode imaging effectively flattened the rough surface, generating a better visual impression of the structure within the surface, and was used for some images along with height mode imaging.

Application of section analysis to the features of the images was used to measure the chain features of SSP (Wada et al., 2003), including length of single molecule, distribution of lengths of molecules, branches and polymers of molecules.

The intervals of aggregates and single molecules were measured by section analysis. In this analysis, the image was sectioned along a line orthogonal to the direction of the samples and the surface profile of the section was plotted. From this surface profile, the width of the sample could be calculated. The length distribution of molecules can be plotted from measures of the single molecules (Wada et al., 2003).

Branched structures were distinguished from overlapping molecules by measuring the heights of the chains. In general the heights of the chains rose by twice when two chains crossed over one another. At genuine branch points the height remained unchanged (Adams, Kroon, Williamson, & Morris, 2003).

The width of a single strand can be calculated by horizontal distance (L) of the software, and the height of the chain by vertical distance (V). The times of the chain widths were recorded as frequency (Fq).

2.6. Statistical analysis

Statistical analyses of vertical distances (V) of chain widths (L) through ANOVA ($P < 0.05$) and Duncan's multiple range tests were performed using SAS 8.0.

3. Results and discussion

3.1. Effects of different atmospheres on SSP structures and aggregates

The high resolution of the AFM has potential for characterizing the heterogeneous structures of SSP, including linear, branching, blocks or polymers.

Fig. 1 shows the AFM images of SSP from fresh peach; most of the SSPs were aggregated, forming large aggregates (C); only a few single linear (D) or small aggregates (shown in Fig. 1(b)) could be viewed.

After storage, the pectin was found to have gradually reduced sizes of the strands and aggregates, as observed by AFM on the 15th day. The AFM images of pectin extracted from CA1 to CA4 are shown in Fig. 2, and from CA5 are in Fig. 3. Small polymers or single linear

molecules can be viewed by AFM. For example, cleavage point (A), branches (B), aggregates (C) and linear single fractions (D), in the CA1group, can be seen in Fig. 2(a). Point D in Fig. 2(d) intuitionally shows linear single fractions releasing from big aggregates; also, the result of CA5 in Fig. 3 was similar. The width of these linear single fractions could be investigated by section analysis.

To determine the molecular lengths, individual molecules were defined as strands that were not entangled with, or overlapping other strands, and which lay entirely within the scanned area (Adams et al., 2003).

Fig. 4 shows CA1 and CA2, while Fig. 5 shows CA3–CA5 of SSP on the 45th day of storage. The length of strands on the 45th day was shorter than that on the 15th day of storage (Figs. 2 and 3). An unexpected structure of a triangle loop was visualized in CA2 of Fig. 4, identified as 'T' in the image (see Fig. 4(d)).

Fig. 6 shows a section analysis (using Fig. 3(b) as example). Studies on SSP at different storage times (Figs. 2, 4 and 5) revealed that the number of branches decreased with storage time. The branches may be detached from the main chain and may have been broken into small fractions by enzymes that could not be viewed by AFM (Decho, 1999).

Decho (1999) reported that scleroglucan had a single-strand polymer with a width of 0.55 nm based on X-ray diffraction measurements. However, the width of scleroglucan was found to be 1 nm by AFM. The differences may be due to the probe-broadening effect or side-by-side association of molecules. Adams et al. (2003) considered that the discrepancy might have partly resulted from formation of the helical structure. The purely geometrical effect can be estimated by calculating the radius (r) of a cylindrical molecule whose measured width (w) is broadened by a tip of radius (R), using the relationship $r = w^2/16R$. Supposing that the measured width of the pectin was ~15 nm and tip radii lay between 20 and 40 nm, a range of molecular rods was calculated between 0.35 and 0.7 nm in radius (Morris et al., 1997).

The aggregates were present even at low dilutions of few single polymers, which suggested that they were not simply superpositions or entanglements of polymers caused by the reduction of solvent volume during drying of the substrate. The characteristic of single polymer was different from multi-polymers (Round et al., 2001).

Polymers aggregated and polymers too small to be exactly visualized by the software were excluded in statistical analysis. The statistical results from dozens of images are shown in Tables 1 and 2. The chain frequencies and V values of different widths of chain (L) on the 15th day storage in CA4 and CA5, and on the 15th and 45th day storage in CA2 are listed. From the two Tables, the probability of smaller L values of chains from normal atmosphere storage was higher than that from the CA4 group (Table 1) and the probabilities were increased with time in the same group (Table 2). However, there were no obvious phenomena for V values.

Table 1
Frequency (Fq) and vertical distances (V) of chain widths (L) on the 15th day under CA4 and CA5 storage

L (nm)	CA4		CA5	
	Fq	V (nm)	Fq	V (nm)
11.719	3	1.267 ± 0.314	9	2.008 ± 0.459
15.625	5	1.659 ± 0.766	9	2.168 ± 0.498
19.531	12	1.246 ± 0.606	4	1.812 ± 0.861
23.438	7	2.325 ± 0.990	7	1.324 ± 0.556
27.344	3	1.731 ± 1.216	1	1.831 ± 0
31.25	3	1.484 ± 0.955	3	1.805 ± 0.687
35.156	1	0.775 ± 0	1	1.513 ± 0
42.969	1	1.162 ± 0	0	0 ± 0
46.875	1	2.635 ± 0	0	0 ± 0
66.406	0	0 ± 0	1	1.752 ± 0

Table 2
Frequency (Fq) and vertical distances (V) of chain widths (L) of CA2 at different storage stages

L (nm)	Initial		15th day		45th day	
	Fq	V (nm)	Fq	L (nm)	Fq	V (nm)
15.625	0	0 ± 0	0	0 ± 0	2	2.295 ± 0.723
17.578	0	0 ± 0	3	2.478 ± 0.316	0	0 ± 0
19.531	0	0 ± 0	0	0 ± 0	4	2.931 ± 0.708
23.438	0	0 ± 0	5	2.066 ± 0.465	6	2.632 ± 0.663
27.344	0	0 ± 0	0	0 ± 0	2	4.91 ± 1.819
29.297	0	0 ± 0	11	2.824 ± 1.018	3	3.468 ± 0.448
31.25	0	0 ± 0	0	0 ± 0	2	4.384 ± 0.827
35.156	3	2.965 ± 0.397	6	3.13 ± 0.616	2	3.734 ± 1.498
41.016	0	0 ± 0	6	3.325 ± 0.597	0	0 ± 0
46.875	3	3.711 ± 0.882	4	3.169 ± 1.419	0	0 ± 0
52.734	0	0 ± 0	5	3.192 ± 0.630	0	0 ± 0
58.594	5	2.989 ± 0.286	3	4.095 ± 1.760	0	0 ± 0
64.453	0	0 ± 0	1	3.208 ± 0	0	0 ± 0
70.313	1	4.84 ± 0	4	3.717 ± 0.931	0	0 ± 0
76.172	0	0 ± 0	2	2.543 ± 0.165	0	0 ± 0
87.891	0	0 ± 0	1	3.365 ± 0	0	0 ± 0

The width of chains from section analysis reflected a group of basic units, with widths of 11.719, 15.625, 19.531 and 17.578 nm, and the widths of other kinds of chains can be summed from these four values. For example, 27.344 nm was the sum of 11.719, 15.625 and 35.156 nm was twice the 17.578 nm.

Throughout the experiments, only two data, 42.926 and 13.672 nm (not shown in Tables), appeared on the 15th day of storage in CA2 and CA5, respectively, and could not be explained by the four units.

3.2. Mechanism of the structure changes of SSP molecules

For the heterogeneous and complex structure, it was hard to explore the changes of pectin structure during

storage. In recent years, many workers have investigated the structure of pectin through specific enzyme actions. Limberg et al. (2000a) compared the actions of p-PME and f-PME. Herbert et al. (2004) proposed that pectin was initially secreted in a highly methylated form and only later became de-esterified within the wall by pectin methyl esterase, and cell wall penetration involved enzyme activity rather than mechanical force. This was in accordance with the results of the fresh SSP sample and most of the SSP molecules were aggregated (Fig. 1(a)).

Massiot, Perron, Baron, and Drilleau (1997) observed that the initial attack of PME was 'endo' and allowed PG action within the galacturonic chain. In our experiments, on the 45th day of storage, many of the SSP molecules were linear without branches. It is necessary to further study whether selective cleavage occurred. Selective cleavage of unesterified galacturonic acid residues allows side chains to be released from the molecule (Needs, Rigby, Ring, & MacDougall, 2001).

In all, many scholars agreed that p-PME caused blockwise de-esterification of pectin, whereas f-PME typically caused random de-esterification (Limberg et al., 2000a; Ridley et al., 2001). Morris et al. (2002) suggested that the decrease in molecular weight was due to chain cleavage by β-elimination and that the increase of reaction time for the neutral protocol resulted in increased cleavage. Ridley et al. (2001) proposed that homogalacturonan and RGII were likely to be covalently linked since they both had backbones composed of 1,4-linked-α-D-Gal*p* A residues and they were both solubilized by treating walls with EPGase. However, many reports have testified that RGI is not linked to other molecules. There is a substantial body of data showing that RGII molecules are covalently cross-linked by borate esters.

In our experiments, the aggregates became gradually smaller with storage time, which indicated that the linkages between SSP molecules were important for the structure and, for different CA groups, the widths of the single linear fractions were different. However, the difference of each inner group was relatively small. Most importantly, almost all of the chain widths were composed of four basic units, of 11.719, 15.625, 19.531 and 17.578 nm, that can be visualized by AFM. This indicated that parallel linkage or intertwist between the basic units was a fundamental characteristic of SSP molecules, most likely between HG and RGII components (Ridley et al., 2001).

4. Conclusions

Controlled atmospheres with lower O_2 and higher CO_2 concentrations significantly inhibited the degradation of SSP of peach, intuitionally visualized by AFM. The size of aggregates, the number of branches, as well as the lengths of single linear chains, decreased with storage time. From the width of chains, almost all of the chains were composed of four basic units: 11.719, 15.625, 19.531 and 17.578 nm, which can be visualized and calculated exactly by AFM. This indicated that parallel linkage or intertwist between the basic units was a fundamental characteristic of SSP molecules.

Acknowledgement

This research was supported by Grants from National Economy and Commerce Committee (Project No. 02CJ-12-07-03).

References

Adams, E. L., Kroon, P. A., Williamson, G., & Morris, V. J. (2003). Characterisation of heterogeneous arabinoxylans by direct imaging of individual molecules by atomic force microscopy. *Carbohydrate Research, 338*, 771–780.

Balnois, E., & Wilkinson, K. J. (2002). Sample preparation techniques for the observation of environmental biopolymers by atomic force microscopy. *Colloids and Surfaces A: Physicochemical and Engineering Aspects, 207*, 229–242.

Chang, C. Y., Lai, I. R., & Chang, W. H. (1995). Relationship between textural changes and the changes in linkages of pectic substances of sweet pepper during cooking processes, and the applicability of the models of interactions between pectin molecules. *Food Chemistry, 53*, 409–416.

Darrort, V., Troyon, M., Ebothé, J., Bissieux, C., & Nicollin, C. (1995). Quantitative study by atomic force microscopy and spectrophotometry of the roughness of electrodeposited nickel in the presence of additives. *Thin Solid Films, 265*, 52–57.

Decho, A. W. (1999). Imaging an alginate polymer gel matrix using atomic force microscopy. *Carbohydrate Research, 315*, 330–333.

Fahlén, J., & Salmén, L. (2003). Cross-sectional structure of the secondary wall of wood fibers as affected by processing. *Journal of Materials Science, 38*, 119–126.

Fernández-Trujillo, J. P., Cano, A., & Artés, F. (2000). Interactions among cooling, fungicide and postharvest ripening temperature on peaches. *International Journal of Refrigeration, 23*, 457–465.

Golovchenko, V. V., Ovodova, R. G., Shashkov, A. S., & Ovodov, Y. S. (2002). Structural studies of the pectic polysaccharide from duckweed Lemna minor L. *Phytochemistry, 60*, 89–97.

Gunning, A. P., Cairns, P., Kirby, A. R., Round, A. N., Bixler, H. J., & Morris, V. J. (1998). Characterising semi-refined *iota*-carrageenan networks by atomic force microscopy. *Carbohydrate Polymers, 36*, 67–72.

Herbert, C., O' Connell, R., Gaulin, E., Salesses, V., Esquerré-Tugayé, M. T., & Dumas, B. (2004). Production of a cell wall-associated endopolygalacturonase by *Colletotrichum lindemuthianum* and pectin degradation during bean infection. *Fungal Genetics and Biology, 41*, 140–147.

Kunzek, H., Kabbert, R., & Gloyna, D. (1999). Aspects of material science in food processing: changes in plant cell walls of fruits and vegetables. *Zeitshrift für Lebensmittel-Untersuchung und-Forschung A, 208*, 233–250.

Limberg, G., Körner, R., Buchholt, H. C., Christensen, T. M., Roepstorff, P., & Mikkelsen, J. D. (2000a). Analysis of pectin structure part 1 – Analysis of different de-esterification mechanisms for pectin by enzymatic fingerprinting using endopectin lyase and endopolygalacturonase II from *Aspergillus niger*. *Carbohydrate Research, 327*, 293–307.

Limberg, G., Körner, R., Buchholt, H. C., Christensen, T. M., Roepstorff, P., & Mikkelsen, J. D. (2000b). Quantification of the amount of galacturonic acid residues in blocksequences in pectin homogalacturonan by enzymatic fingerprinting with exo- and endo-polygalacturonase II from *Aspergillus niger*. *Carbohydrate Research, 327*, 321–332.

Massiot, P., Perron, V., Baron, A., & Drilleau, J. F. (1997). Release of methanol and depolymerization of highly methyl esterified apple pectin with an endopolygalacturonase from *Aspergillus niger* and pectin methylesterases from *A. niger* or from orange. *Lebensmittel-Wissenschaft und-Technologie, 30*, 697–702.

Morris, G. A., Hromádková, Z., Ebringerová, A., Malovíková, A., Alföldi, J., & Harding, S. E. (2002). Modification of pectin with UV-absorbing substitutents and its effect on the structural and hydrodynamic properties of the water-soluble derivatives. *Cabohydrate Polymers, 48*, 351–359.

Morris, V. J., Gunning, A. P., Kirby, A. R., Round, A., Waldron, R. K., & Ng, A. (1997). Atomic force microscopy of plant cell walls, plant cell wall polysaccharides and gels. *International Journal of Biological Macromolecules, 21*, 61–66.

Morris, V. J., Mackie, A. R., Wilde, P. J., Kirby, A. R., Mills, E. C. N., & Gunning, P. (2001). Atomic force microscopy as a tool for interpreting the rheology of food biopolymers at the molecular level. *Lebensmittel-Wissenschaft und-Technologie, 34*, 3–10.

Needs, P. W., Rigby, N. M., Ring, S. G., & MacDougall, A. J. (2001). Specific degradation of pectins via a carbodiimide-mediated Lossen rearrangement of methyl esterified galacturonic acid residues. *Carbohydrate Research, 333*, 47–58.

Reed, J., Singer, E., Kresbach, G., & Schwartz, D. C. (1998). A quantitative study of optical mapping surfaces by atomic force microscopy and restriction endonuclease digestion assays. *Analytical Biochemistry, 259*, 80–88.

Ridley, B. L., O' Neill, M. A., & Mohnen, D. (2001). Pectins: structure, biosynthesis, and oligogalacturonide-related signaling. *Phytochemistry, 57*, 929–967.

Round, A. N., MacDougall, A. J., Ring, S. G., & Morris, V. J. (1997). Unexpected branching in pectin observed by atomic force microscopy. *Carbohydrate Research, 303*, 251–253.

Round, A. N., Rigby, N. M., MacDougall, A. J., Ring, S. G., & Morris, V. J. (2001). Investigating the nature of banching in pectin by atomic force microscopy and carbohydrate analysis. *Carbohydrate Research, 331*, 337–342.

Tijskens, L. M. M., Rodis, P. S., Herbog, M. L., Kalantzi, U., & Dijk, C. (1998). Kinetics of polygalacturonase activity and firmness of peaches during storage. *Journal of Food Engineering, 35*, 111–126.

Wada, H., Usekura, H., Sugawara, M., Katori, Y., Kakehata, S., Ikeda, K., et al. (2003). Relationship between the local stiffness of the outer hair cell along the cell axis and its ultrastructure observed by atomic force microscopy. *Hearing Research, 177*, 61–70.

Willats, W. G. T., Limberg, G., Buchholt, H. C., Alebeek, G., Bensen, J., Christensen, T. M., et al. (2000). Analysis of pectic epitopes recognised by hybridoma and phage display monoclonal antibodies using defined oligosaccharides, polysaccharides, and enzymatic degradation. *Carbohydrate Research, 327*, 309–320.

Zhou, H. W., Sonego, L., Khalchitski, A., Ben-Arie, R., Lers, A., & Lurie, S. (2000). Cell wall enzymes and cell wall changes in 'Flavortop' Nectarines: mRNA abundance, enzymes activity, and changes in pectic and neutral polymers during ripening and in wolly fruit. *Journal of the American Society for Horticultural Science, 125*, 630–637.